Nonlinear Electrodynamics of Superconducting Films

K. ROSE* AND M. D. SHERRILL
General Electric Research and Development Center, Schenectady, New York
(Received 20 December 1965)

Microwave-transmission measurements at 9.4 Gc/sec over a wide range of incident power have been used to study the nonlinear electrodynamics of thin superconducting films. By measuring the amplitude and phase of the fundamental transmitted field, the contributions of superelectrons and normal electrons to the electrodynamics of the films have been determined. In low microwave fields the nonlinear behavior of the films can be attributed to the breakup of superconducting pairs in agreement with the Ginzberg-Landau theory. In high microwave fields, regions of normal resistance appear through which a dc bias current cannot avoid passing. Most of the third-harmonic power is generated by these resistive regions.

I. INTRODUCTION

MANY problems associated with the time-dependent behavior of superconductors remain unsolved and a complete understanding of the creation and destruction of the superconducting state is lacking.[1] A number of authors have discussed theories of the nonlinear behavior of superconductors in the presence of magnetic fields and in the presence of transport currents or superfluid flow.[2–5] Experimentally, there has been substantial progress in our understanding of the influence of the magnetic field on the behavior of type-I and type-II superconductors.[6–10] An understanding of the influence of superfluid flow on the superconducting state has developed more slowly, principally as a result of experimental difficulties.[11] Our experimental technique allows us to measure the effects of superfluid flow on the superconducting state and gives some insight into its time-dependent properties. The present measurements of the amplitude and phase of the 9.4-Gc/sec waves transmitted through superconducting films agree with earlier measurements which showed that thin superconducting films exhibit a transmission which is a function of microwave power, and produce harmonics of the microwave field.[12]

Related measurements have been made by several workers. The transition-time experiments of Nethercott and von Gutfield[13] and the observation of parametric amplification by Clorfeine[14] depend upon the nonlinear electrodynamics of superconducting films. Measurements by Mitescu[15] using the technique of Mercereau and Crane[16] did not show the dependence of superelectron density on pair velocity predicted by the Ginzburg-Landau theory. Recent microwave measurements of the change in the reactive component of a superconductor's conductivity with dc bias currents show agreement with the temperature dependence of the Ginzburg-Landau theory in the limit of zero-pair velocity.[17,18] Our experiments indicate the dependence of superelectron density on pair velocity and agree with the Ginzburg-Landau theory at low-power levels.

Studies of the influence of superfluid flow on the superconducting state are best made on specimens which are small compared with the coherence distance so that v_s, the pair velocity, may be assumed constant throughout the specimen.[2] Making measurements on thin films allows us to assume that v_s is constant through the film which greatly simplifies both the analysis of the experiments and their theoretical interpretation. Because the films are thin, their normal resistance per square is large. This leads to a large, easily measured change in impedance when the films make a transition to the normal state. Since the critical currents that a thin film can support are low, the application of relatively small microwave fields can induce a change of state.

In Sec. II of this article, we describe our experimental techniques. Section III shows that measuring the amplitude and phase of the fundamental transmitted wave allows us to separate the contributions of superelectrons and normal electrons to the behavior of the film. The experimental method is valid at all power levels although the theoretical interpretation of the results requires modification at higher power levels. There is a low-power region where the nonlinearity is weak and the behavior of the film can be described by a

* Present address: Rensselaer Polytechnic Institute, Troy, New York.

[1] A. B. Pippard, Rev. Mod. Phys. **36**, 328 (1964).
[2] J. Bardeen, Rev. Mod. Phys. **34**, 667 (1962).
[3] K. T. Rogers, Ph.D. thesis, University of Illinois, 1960 (unpublished).
[4] C. D. Mitescu, Bull. Am. Phys. Soc. **7**, 609 (1962).
[5] R. H. Parmenter, RCA Rev. **26**, 323 (1962).
[6] D. E. Morris and M. Tinkham, Phys. Rev. **134**, A1154 (1964).
[7] D. H. Douglass, Jr., and L. M. Falicov, in *Progress in Low Temperature Physics*, edited by C. J. Gorter (North-Holland Publishing Company, Amsterdam, 1964), Vol. 4, p. 97.
[8] M. J. Stephen and J. Bardeen, Phys. Rev. Letters **14**, 112 (1965).
[9] Y. B. Kim, Bull. Am. Phys. Soc. **10**, 302 (1965).
[10] B. Rosenblum, Bull. Am. Phys. Soc. **10**, 302 (1965).
[11] P. Fulde and R. A. Ferrell, Bull. Am. Phys. Soc. **10**, 302 (1965).
[12] M. D. Sherrill and K. Rose, Rev. Mod. Phys. **36**, 312 (1964).
[13] A. H. Nethercott and R. J. von Gutfield, Phys. Rev. **131**, 576 (1963).
[14] A. S. Clorfeine, Appl. Phys. Letters **4**, 131 (1964).
[15] C. D. Mitescu, Rev. Mod. Phys. **36**, 305 (1964).
[16] J. E. Mercereau and L. T. Crane, Phys. Rev. Letters **9**, 381 (1962).
[17] J. I. Gittleman and B. Rosenblum, Proc. IEEE **52**, 1138 (1964).
[18] J. I. Gittleman, B. Rosenblum, T. Seidel, and A. Wicklund, Phys. Rev. **136**, A527 (1965).

two-fluid model as well as a higher power region where the nonlinearity is substantial and a two-fluid description breaks down. These are the "depairing" and "domain-growth" regions discussed in Sec. V.

II. EXPERIMENTAL TECHNIQUE

A. Film Characteristics

The tin films used in these experiments were condensed at room temperature on fused quartz substrates. Four gold patches on the substrate were provided for monitoring the film resistance. To reduce agglomeration a very thin nonconducting gold layer was deposited on the substrate before the tin evaporation. This made it possible to produce the thin high-resistance films required by the experiment. Films produced in this way were quite sturdy. Upon initial exposure to air their resistance increased usually by a few percent. They subsequently survived exposures to air, cyclings between room temperature and 4°K, and storage for periods of several months in a desiccator without marked change in resistance, transition temperature, or high-frequency properties.

The film resistances per square at 4°K varied from about 10 Ω to about 240 Ω. The ratio of their resistances at room temperature to their resistances at helium temperature ranged from about 2 to about 8. This ratio depended markedly upon the evaporation time, which ranged from about 2–15 min, and the pressure in the evaporator bell during evaporation, which was usually about 10^{-6} mm Hg. Films evaporated in shorter times and at lower pressures had higher resistance ratios. The transition temperatures of the films studied ranged from 2.9–3.8°K. The quantity of gold deposited prior to the tin evaporation was the principal cause of the depression of the transition temperature. The temperature range in which the films lost 90% of their resistance, which we define as the width of the superconducting transition, varied from 0.02°K to about 0.15°K. The films with higher transition temperatures in general exhibited narrower transitions.

Table I gives the detailed characteristics of three films on which amplitude and phase measurements were made. A lower limit for the film thickness was estimated from the temperature dependence of the resistance.[19] The thickness and residual normal resistance give a lower limit for a Ginzburg-Landau κ[20] which is greater than $2^{-1/2}$ for the films we have studied.

B. Microwave Circuit

The microwave bridge circuit shown in Fig. 1 was used to determine the amplitude and phase of the fundamental component of the transmitted wave relative to the incident wave. In these measurements a wave coming directly from the klystron was added to the wave transmitted through the film. The attenuator (A_2) and phase shifter (P) were set to obtain a null at the balanced detector (D) for each setting of the input attenuator (A_1). To minimize heating of the film and harmonics in the incident field a pulsed klystron was used as a source of microwave power. Measurements were made at a frequency of 9.4 Gc/sec using 2-μsec microwave pulses of up to 12 W peak power repeated 100 or 1000 times/sec.

The films were mounted to cover the waveguide cross section using indium seals to reduce the amount of power leaking around the film. Leakage seems to be the principal source of error in these measurements and particular care must be taken to avoid leakage at low temperatures. In some cases, when proper precautions were not taken, transmission anomalies have been observed which could be explained by the influence of a leakage path. (This was true of the scribed films described in Sec. VB.)

The waveguide and film were cooled by placing them in direct contact with liquid helium inside the cryostat. To reduce the effects of harmonics on measurements at the fundamental frequency both the klystron and film were followed by Kearfott isolators which acted as matched loads for harmonics of the fundamental frequency. To measure the third harmonic power produced by the film, the isolator following the film was removed and the film was terminated by a Narda 730 attenuator followed by a tapered waveguide, attenuator, and crystal detector. The Narda attenuator could be set to attenuate the fundamental wave by more than 20 dB while attenuating the third harmonic wave by less than 2 dB. In this way the effects of strong reflections of the fundamental wave from the taper were eliminated.

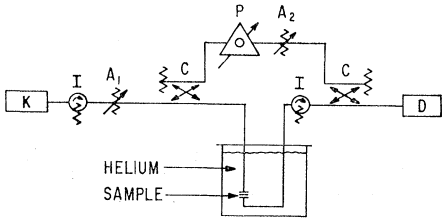

FIG. 1. Schematic diagram of the microwave bridge circuit used in the experiments. Pulsed klystron, K; isolators, I; precision attenuators, A_1 and A_2; directional couplers, C; precision phase shifter, P; balanced detector, D.

TABLE I. Film properties.

Film	Film resistance (Ω/sq) 293°K	77°K	4°K	Thickness (Å)	Ginzberg-Landau parameter κ	T_c (°K)	ΔT_c (°K)
1	306	178	138	≈8	2.8	3.66	0.05
2	309	173	122	≈8	3.2	3.61	0.05
3	526	···	239	≈5	3.6	3.63	0.09

[19] J. Niebuhr, Z. Physik 132, 468 (1952).
[20] E. A. Lynton, *Superconductivity* (John Wiley & Sons, Inc., New York, 1962), p. 67.

III. THEORY OF MEASUREMENT

In these experiments a TE_{10}-mode microwave field is incident upon a thin superconducting film covering the waveguide cross section. Since the film is thin compared with the superconducting penetration depth, the current density and electric-field strength are constant through the film thickness. For small incident fields the film behaves linearly, and this condition may be combined with the requirement that the discontinuity in the transverse component of magnetic field equal the surface current density to give one boundary condition

$$Jd=(2/Z)(E_i-E_t) \tag{1}$$

if we assume that the generator and load are matched to the waveguide. Here J is the film current density, d is the film thickness, $E_i=E_0\sin(\pi x/a)\exp(i\omega t)$ is the incident electric field, E_t is the transmitted electric field, Z is the TE_{10} guide impedance, and a is the width of the waveguide. Under these conditions E_t, the transmitted field, is the electric field across the film.

In general, E_t will differ from E_i in amplitude and phase, and in the linear case one can relate the current through the film to the electric field across the film by introducing a complex conductivity, $\sigma_1-i\sigma_2$.

$$J=(\sigma_1-i\sigma_2)E_t. \tag{2}$$

In the normal state $J=\sigma_N E_t$. One can calculate σ_1/σ_N and σ_2/σ_N from the boundary condition by measuring $Te^{i\varphi}=E_t/E_i$, the transmission (T) and phase shift (φ), relative to their values when the film is in the normal state.

When the incident field is large the relationship between J and E_t is nonlinear so that we must consider all modes and harmonics of the transmitted field that can be coupled to the incident field by the film. Thus, only the TE_{m0} modes are needed to describe the spatial variation because the sample geometry does not permit coupling to other modes. To account for both modes and harmonics E_t and J need to be expanded in a double Fourier series. Using the boundary condition that the electric field is constant through the film thickness ($E_i+E_r=E_t$), the reflected field can be eliminated from the boundary condition on the magnetic fields and we obtain one boundary condition similar to Eq. (1).

$$\sum_{m=1}^{\infty}\sum_{n=1}^{\infty}\sin(m\pi x/a)(J_{mn}{}^{s}\sin n\omega t+J_{mn}{}^{c}\cos n\omega t)d=\frac{2}{Z_{11}}E_0{}^{c}\sin\frac{\pi x}{a}\cos\omega t+\frac{2}{Z_{11}}E_0{}^{s}\sin\frac{\pi x}{a}\sin\omega t$$
$$-\sum_{\substack{m=1\\ \text{for}\\ m\lambda_n<2a}}^{\infty}\sum_{n=1}^{\infty}\frac{2}{Z_{mn}}\sin\frac{m\pi x}{a}(E_{T_{mn}}{}^{s}\sin n\omega t+E_{T_{mn}}{}^{c}\cos n\omega t)$$
$$-\sum_{\substack{m=1\\ \text{for}\\ m\lambda_n>2a}}^{\infty}\sum_{n=1}^{\infty}\frac{2}{Z_{mn}}\sin\frac{m\pi x}{a}(E_{T_{mn}}{}^{c}\sin n\omega t-E_{T_{mn}}{}^{s}\cos n\omega t). \tag{3}$$

Here the complex notation has been abandoned because it is not useful in a nonlinear situation. The incident field is $\sin(\pi x/a)[E_0{}^{c}\cos\omega t+E_0{}^{s}\sin\omega t]$. The coefficients Z_{mn} are the magnitudes of the characteristic waveguide impedances for waves of angular frequency $n\omega$ in the TE_{m0} mode. The superscripts s and c indicate that these coefficients correspond to sine and cosine time variations in J and E_t. The summation on the right is written in two parts because the only fields which can propagate in the TE_{m0} mode are those whose free-space wavelength, $\lambda_n=2\pi c/n\omega$, is less than $2a/m$. Fields for which $m\lambda_n>2a$ are termed evanescent and decay exponentially with distance from the film. Further, as the interchange of sine and cosine coefficients in the last term of Eq. (2) indicates, E and H are out of phase by $\pi/2$ for these waves so that their time-average Poynting vector vanishes.

Since all of the functions in Eq. (3) with different m or n are orthogonal, we can separate terms to obtain a set of equations for the coefficients.

$$J_{11}{}^{c}d=(2/Z_{11})(E_0{}^{c}-E_{T11}{}^{c}),$$
$$J_{11}{}^{s}d=(2/Z_{11})[E_0{}^{s}-E_{T11}{}^{s}],$$
$$J_{mn}{}^{c}d=\left\{\begin{matrix}-(2/Z_{mn})E_{T_{mn}}{}^{c}\text{ for }m\lambda_n<2a\\ -(2/Z_{mn})E_{T_{mn}}{}^{s}\text{ for }m\lambda_n>2a\end{matrix}\right\}n\neq1,\ m\neq1, \tag{4}$$
$$J_{mn}{}^{s}d=\left\{\begin{matrix}-(2/Z_{mn})E_{T_{mn}}{}^{s}\text{ for }m\lambda_n<2a\\ +(2/Z_{mn})E_{T_{mn}}{}^{c}\text{ for }m\lambda_n>2a\end{matrix}\right\}n\neq1,\ m\neq1.$$

From these equations we see that a measurement of the amplitude and phase of any component of the electric field relative to the incident wave determines the corresponding Fourier component of the film current. To completely specify the current it would be necessary to make such measurements for every Fourier component. In practice this is very difficult except for

the fundamental component ($m=n=1$) which will propagate in the TE_{10} mode only. The evanescent fields ($m\lambda_n>2a$) will not propagate to the detector at all, while the higher frequency fields ($n\geq 2$) can propagate in the guide in more than one mode, each with a different guide wavelength. This means that phase measurements on the higher frequency fields by a distant detector would be extremely unreliable. However it is possible to measure the total power in the transmitted field at any frequency $n\omega$. Reference 12 reports such measurements at the third harmonic frequency, and shows that no detectable second-harmonic power is generated.

In deriving Eqs. (4) only relative phase has been specified. We are therefore free to set the coefficient of our choice equal to zero. A convenient choice is $E_{T_{11}}{}^s=0$ so that the fundamental transmitted field becomes $E_{tf}=E_{T_{11}}{}^c \sin(\pi x/a)\cos\omega t$ and the phases of other fields and currents are measured with respect to this wave. With this choice we may write

$$J_f=E_{T_{11}}{}^c(J_{11}{}^c/E_{T_{11}}{}^c)\sin(\pi x/a)\cos\omega t + E_{T_{11}}{}^c(J_{11}{}^s/E_{T_{11}}{}^c)\sin(\pi x/a)\sin\omega t.$$

The ratios in parentheses are uniquely determined by the measurements. We therefore *define* the *fundamental conductivity*

$$\sigma_{1f}=J_{11}{}^c/E_{T_{11}}{}^c;\ \sigma_{2f}=J_{11}{}^s/E_{T_{11}}{}^c. \tag{5}$$

In the complex notation of Eq. (2) this is

$$J_f=(\sigma_{1f}-i\sigma_{2f})E_{tf}.$$

This ratio is not, strictly speaking, a conductivity since in the nonlinear region the fundamental component of the current results from the entire electric field rather than the fundamental field alone. It is, however, well defined even when the instantaneous conductivity varies during a cycle. In the limit of low incident power it is identical to the complex conductivity defined by Eq. (2) and the measurements will show that at very high power σ_{2f} approaches zero and σ_{1f} approaches σ_N.

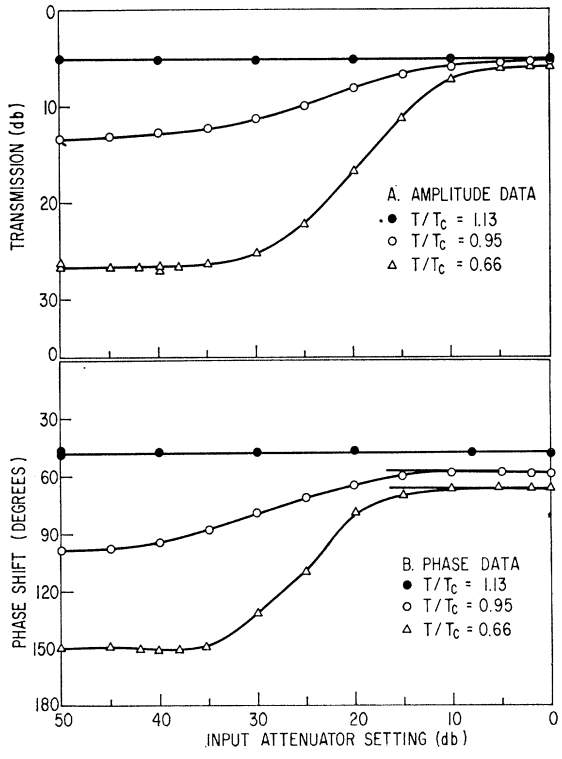

FIG. 2. Experimental measurements on film 2 of Table I. (a). Dependence of fundamental transmission on incident power. (b). Dependence of phase shift in transmitted fundamental field on incident power.

IV. EXPERIMENTAL RESULTS

The experimental results for one film at different temperatures are shown in Fig. 2. The measured transmission and phase shift are shown as a function of incident power level. Note that above T_c where the film is in the normal state both the transmission and phase are independent of input power as one would expect. Below T_c, the transmission varies with incident power as reported earlier.[12] A constant transmission at low incident powers when the film is in the superconducting state is followed by a transition to a constant transmission corresponding to the normal state at high incident powers. The phase shift exhibits similar behavior. The apparent shift in phase with temperature at high power seems to be caused by the change in helium level in the waveguide.

From this data one can obtain values for σ_{1f}/σ_N and σ_{2f}/σ_N from the results of the previous section by taking the phase shift as zero when the film is in the normal state. Figure 3 shows the low-temperature variation of fundamental conductivity normalized to σ_2 with fundamental transmitted power ($|P_{tf}|=T_f{}^2|P_i|$) for the films whose characteristics are given in Table I. The range of transmitted power shown in Fig. 3 corresponds to only the lower part of the range of incident power shown in Fig. 2. Since the nonlinearity occurs at a different absolute power for each film at each temperature, the curves are plotted as a function of *relative* transmitted power. This amounts to normalizing the critical current to the same value in each case.

The lossless component σ_{2f} decreases monotonically with transmitted power, while the lossy component σ_{1f} increases from a very low value to a maximum and then decreases to σ_N. For convenience of interpretation, σ_{1f} and σ_{2f} have been normalized to σ_2 which is the low-power limit of σ_{2f}. Note that with this normalization σ_{1f} and σ_{2f} agree quite well for all the films, although the values of σ_2/σ_N and normal resistance differ substantially. To prepare the way for later interpretations we note that at low powers the behavior of the film is

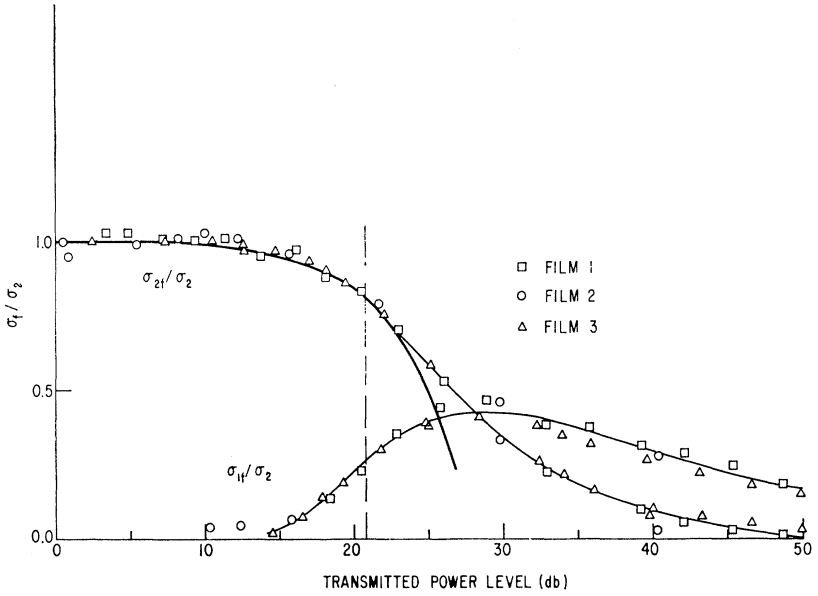

FIG. 3. The electric field dependence of the fundamental conductivity. The heavy curve shows the variation of σ_{2f}/σ_2 derived from the Ginzburg-Landau theory. At the vertical dashed line the supercurrent amplitude approximately equals the theoretical critical current. Films are listed in Table I. Film 1, $T/T_c=0.57$, $\sigma_2/\sigma_N=7.5$; film 2, $T/T_c=0.66$, $\sigma_2/\sigma_N=16.0$; film 3, $T/T_c=0.51$, $\sigma_2/\sigma_N=16.5$.

dominated by the decrease of σ_{2f}, while at higher powers its behavior is dominated by the maximum in σ_{1f}.

In addition to measurements at the fundamental frequency we have measured the third-harmonic power generated by these films and their dc resistance during the microwave pulses. The harmonic measurements agree with those reported in Ref. 12. The dc measurements are compared with the microwave results at both the fundamental and third harmonic frequencies in Sec. VB.

In the course of the measurements of nonlinear effects reported here, we have made some measurements of the temperature dependence of the linear conductivity. The measured temperature dependences of σ_1/σ_N and σ_2/σ_N agree qualitatively with temperature dependences calculated on the basis of the BCS theory.[21] The forms of the curves are similar in the two cases and the peak value of σ_1/σ_N is the right size (1.4 to 1.6), but, as the temperature decreases, σ_1/σ_N falls off more sharply and σ_2/σ_N rises more slowly than theory predicts. In Fig. 4 the experimental results for one film are compared with calculations based on the BCS theory for two values of the parameter $a=\Delta_0/kT_c$. These linear results are of a preliminary nature and require further experimentation before conclusions are drawn from the data.

V. INTERPRETATION

The results presented here suggest that two distinct mechanisms combine to determine the nonlinear behavior of these films. The first of these is the loss of superelectrons from the superfluid as the supervelocity v_s increases. This accounts for the initial decrease of σ_{2f} with power and is the dominant mechanism where the nonlinearity is small. The second is the production of normal domains which the current cannot avoid. This mechanism accounts for the large lossy component σ_{1f} and is the dominant mechanism at higher powers. It is the rapid production and collapse of this domain structure which produces most of the observed third-harmonic power.

A. Low-Power Region ("Superelectron Depairing")

Under the influence of an electric field the common velocity of electron pairs v_s increases according to the

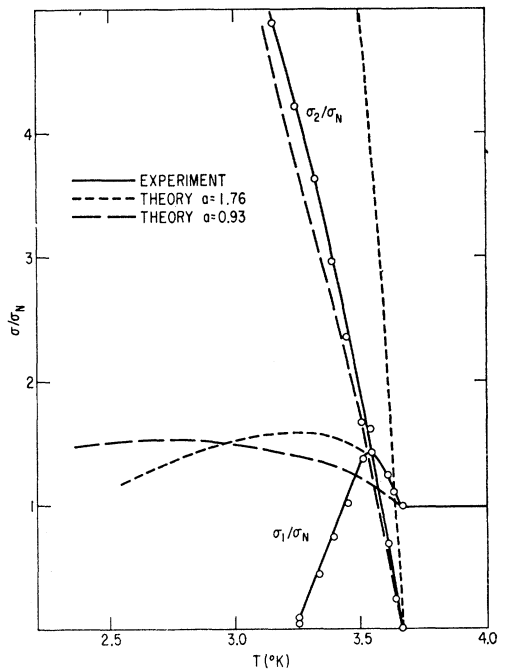

FIG. 4. Temperature dependence of complex conductivity for film 1 of Table I compared with calculations based on the BCS theory. $a=\Delta_0/kT_c$.

[21] P. B. Miller, Phys. Rev. 118, 928 (1960).

relation

$$dv_s/dt=(e/m)E. \tag{6}$$

For films thin compared with a penetration depth the Ginzburg-Landau theory predicts that under equilibrium conditions n_s, the density of superelectrons, must decrease with increasing superelectron velocity in order to minimize the free energy.[2] This breakup of superelectron pairs results in a supercurrent density J_2, given by

$$J_2=n_s ev_s=n_s(0)[1-\tfrac{1}{3}(v_s/v_m)^2]ev_s. \tag{7}$$

$n_s(0)$ is the superelectron density at zero current and v_m is the value of v_s for which J_2 is a maximum, $J_c=\frac{2}{3}n_s(0)ev_m$. J_c is the critical current density of the film.[2] Although the Ginzburg-Landau theory was derived for temperatures near T_c, Eq. (7) agrees with calculations based on the BCS theory for temperatures above $0.4T_c$.[2] Below $0.4T_c$ these calculations predict a decrease of n_s with v_s which is larger than Eq. (7) predicts for v_s approaching v_m. We have not attempted to compare our results with Parmenter's theory of the nonlinear electrodynamics of the superconducting state because of the complexity of the calculations that would be involved.[5,22] Nonetheless, such a comparison could be made and presents an area for further study.

Equation (7) should describe the nonlinear behavior of the superfluid, provided the electric field is so small that the energy dissipated by the normal fluid is much less than the kinetic energy of the superfluid and dv_s/dt is so small that the superelectrons can assume an equilibrium distribution.[2] The nonlinear electrodynamics of a superconducting film across a waveguide can be described then by combining Eqs. (3), (6), and (7). This results in a set of coupled nonlinear differential equations which would be quite difficult to solve for arbitrary values of electric field. Fortunately, a good approximation to the solution can be found which is easy to compute and should be valid for $|v_s|\leq v_m$.

Our experimental measurements indicate that, consistent with Eq. (7), only odd harmonics are produced, and we expect that the current in the film will be distributed symmetrically with respect to the center of the waveguide so that only odd modes will be excited. We may write the transmitted field as

$$\begin{aligned}E_t=&\alpha(J_m/\sigma_2)\sin(\pi x/a)\cos\omega t+E_{T_{13}{}^c}\sin(\pi x/a)\cos 3\omega t\\&+E_{T_{13}{}^s}\sin(\pi x/a)\sin 3\omega t+E_{T_{31}{}^c}\sin(3\pi x/a)\cos\omega t\\&+E_{T_{31}{}^s}\sin(3\pi x/a)\sin\omega t+E_{T_{33}{}^c}\sin(3\pi x/a)\cos 3\omega t\\&+E_{T_{33}{}^s}\sin(3\pi x/a)\sin 3\omega t\cdots.\end{aligned} \tag{8}$$

Here we have expressed $E_{T_{11}{}^c}$ as

$$E_{T_{11}{}^c}=\alpha(J_m/\sigma_2)=\alpha(m\omega/e)v_m,$$

where $\sigma_2=n_s(0)e^2/m\omega$, and $J_m=n_s(0)ev_m$. With $E_{T_{11}{}^c}$ expressed in this way the fundamental component of v_s is $\alpha v_m\sin(\pi x/a)\sin\omega t$. The approximations made in the calculations which follow will be adequate for $\alpha\leq 1$.

If we substitute Eq. (8) for the electric field into Eq. (6) and integrate we obtain v_s.

$$\begin{aligned}v_s=(e/m\omega)[&\alpha(J_m/\sigma_2)\sin(\pi x/a)\sin\omega t\\&+\tfrac{1}{3}E_{T_{13}{}^c}\sin(\pi x/a)\sin 3\omega t-\tfrac{1}{3}E_{T_{13}{}^s}\sin(\pi x/a)\cos 3\omega t\\&+E_{T_{31}{}^c}\sin(3\pi x/a)\sin\omega t-E_{T_{31}{}^s}\sin(3\pi x/a)\cos\omega t\\&+\tfrac{1}{3}E_{T_{33}{}^c}\sin(3\pi x/a)\sin 3\omega t\\&-\tfrac{1}{3}E_{T_{33}{}^s}\sin(3\pi x/a)\cos 3\omega t+\cdots].\end{aligned}$$

We substitute this expression for v_s into Eq. (7), expand, and drop terms containing squares and cubes of the higher order fields as factors.

$$\begin{aligned}J_2=&\left\{\alpha J_m-\frac{\sigma_2}{16}\alpha^2\left[3\alpha\frac{J_m}{\sigma_2}-E_{T_{13}{}^c}-3E_{T_{31}{}^c}+\tfrac{1}{3}E_{T_{33}{}^c}\right]\right\}\sin\frac{\pi x}{a}\sin\omega t-\tfrac{1}{16}\sigma_2\alpha^2[E_{T_{13}{}^s}+E_{T_{31}{}^s}-\tfrac{1}{3}E_{T_{33}{}^s}]\sin\frac{\pi x}{a}\cos\omega t\\&-\tfrac{1}{3}\sigma_2E_{T_{13}{}^s}\sin\frac{\pi x}{a}\cos 3\omega t+(\tfrac{1}{3}\sigma_2E_{T_{13}{}^c}+\tfrac{1}{16}\alpha^3J_m)\sin\frac{\pi x}{a}\sin 3\omega t-\sigma_2E_{T_{31}{}^s}\sin\frac{3\pi x}{a}\cos\omega t\\&+(\sigma_2E_{T_{31}{}^c}+\tfrac{1}{16}\alpha^3J_m)\sin\frac{3\pi x}{a}\sin\omega t+(\tfrac{1}{3}\sigma_2E_{T_{33}{}^c}-(1/48)\alpha^3J_m)\sin\frac{3\pi x}{a}\sin 3\omega t-\tfrac{1}{3}\sigma_2E_{T_{33}{}^s}\sin\frac{3\pi x}{a}\cos 3\omega t\cdots.\end{aligned} \tag{9}$$

Applying the boundary conditions Eqs. (6) to the last six terms of Eq. (9) gives

$$\begin{aligned}J_{13}{}^cd&=-\tfrac{1}{3}\sigma_2dE_{T_{13}{}^s} &&=-(2/Z_{13})E_{T_{13}{}^c},\\J_{13}{}^sd&=\tfrac{1}{3}\sigma_2dE_{T_{13}{}^c} &&+\tfrac{1}{16}d\alpha^3J_m=-(2/Z_{13})E_{T_{13}{}^s},\\J_{31}{}^cd&=-\sigma_2dE_{T_{31}{}^s} &&=-(2/Z_{31})E_{T_{31}{}^s},\\J_{31}{}^sd&=\sigma_2dE_{T_{31}{}^c} &&+\tfrac{1}{16}d\alpha^3J_m=+(2/Z_{31})E_{T_{31}{}^c},\\J_{33}{}^cd&=-\tfrac{1}{3}\sigma_2dE_{T_{33}{}^s} &&=-(2/Z_{33})E_{T_{33}{}^c},\\J_{33}{}^sd&=\tfrac{1}{3}\sigma_2dE_{T_{33}{}^c} &&-(1/48)d\alpha^3J_m=-(2/Z_{33})E_{T_{33}{}^s}.\end{aligned}$$

Except for temperatures very near T_c, $\sigma_2d\gg 2/Z_{nm}$ so that:

$$\begin{aligned}E_{T_{13}{}^c}&\cong-\frac{3}{16}\frac{\alpha^3}{\sigma_2}J_m=-\frac{3}{16}\alpha^2E_{T_{11}{}^c},\\E_{T_{33}{}^c}&\cong\frac{1}{16}\frac{\alpha^3}{\sigma_2}J_m=\frac{1}{16}\alpha^2E_{T_{11}{}^c},\\E_{T_{31}{}^c}&\cong-\frac{1}{16}\frac{\alpha^3}{\sigma_2}J_m=-\frac{1}{16}\alpha^2E_{T_{11}{}^c},\\E_{T_{13}{}^c}&\gg E_{T_{13}{}^s}\cong 0,\\E_{T_{33}{}^c}&\gg E_{T_{33}{}^s}\cong 0,\\E_{T_{31}{}^c}&\gg E_{T_{31}{}^s}\cong 0.\end{aligned} \tag{10}$$

[22] R. H. Parmenter and L. J. Berton, RCA Rev. 25, 596 (1964).

So we have a TE_{10}-mode third-harmonic field $E_{T_{13}}{}^c$, a TE_{30}-mode third-harmonic field $E_{T_{33}}{}^c$, and a nonpropagating or evanescent TE_{10} field $E_{T_{31}}{}^c$, each proportional to the cube of the fundamental TE_{10} field.

Now, by substituting the expressions (10) into the first two terms of Eq. (9) we obtain the fundamental component of the current as a function of the fundamental field.

$$J_{2f}=\alpha J_m\left[1-\tfrac{3}{16}\alpha^2\left(1+\frac{19}{144}\alpha^2\right)\right]\sin\frac{\pi x}{a}\sin\omega t$$

$$=\sigma_2 E_{T_{11}}{}^c\left[1-\tfrac{3}{16}\alpha^2\left(1+\frac{19}{144}\alpha^2\right)\right]\sin\frac{\pi x}{a}\sin\omega t. \qquad (11)$$

This current which comes from the first term of Eq. (9) is lossless and out of phase with the field by $\frac{1}{2}\pi$. The lossy current represented by the second term in Eq. (9) is very small and taken as zero in our present approximation. It results because the generation of higher order fields appears as a loss to the fundamental wave.

We may use the definition of the fundamental conductivity, Eq. (5), to obtain

$$\sigma_{2f}/\sigma_2=\left[1-\tfrac{3}{16}\alpha^2(1+(19/144)\alpha^2)\right]\cong 1-\tfrac{3}{16}\alpha^2. \qquad (12)$$

We recall that $\alpha=(e/m\omega v_m)E_{T_{11}}{}^c$ so that α^2 is proportional to the fundamental transmitted power. The term in α^4 results from mixing with the higher order fields and the error in σ_{2f} introduced by dropping it is only 2.5% for $\alpha=1$. Since the approximations used in deriving Eq. (12) are valid only for $\alpha\leq 1$ we shall use the simpler expression for comparison with the experimental results.

Equation (12) is shown as the heavy solid line in Fig. 3. The vertical dashed line indicates the point at which $\alpha=1$ so that the fundamental component of v_s is $v_m\sin(\pi x/a)\sin\omega t$ and the amplitude of J_2 is approximately J_c. Until this current is reached the calculated σ_{2f} agrees well with the measurements. At higher powers σ_{2f} falls off more slowly than the solid curve even though an exact solution of Eq. (7) would result in an even more rapid decrease of σ_{2f} for $\alpha>1$. So we see that superconductivity disappears less abruptly and persists in much higher fields than Eq. (7) predicts.

The measured value of $|J_{2f}|=\sigma_{2f}E_{T_{11}}{}^c$ is an ever-increasing function of the fundamental transmitted field. This indicates that the decrease in the magnitude of the supercurrent with $|v_s|$ and E_{tf} which is the most striking feature of Eqs. (7) and (9) is not observed. Because of the low impedance of superconducting films, this decrease is difficult to measure. Since the waveguide impedance is much larger than $(\sigma_2 d)^{-1}$ it is not possible for the transmitted field to follow the superconducting characteristic defined by Eq. (7); however, the result of a decrease in $|J_2|$ should be observable as a decrease in $|J_{2f}|$.

Since Eq. (7) was derived under the assumption that the energy dissipation in the normal fluid could be neglected in comparison with the kinetic energy of the superfluid, it does not predict the variation of σ_{1f} with transmitted power. At low temperatures and powers σ_{1f} is indeed small compared with σ_{2f} and is difficult to measure. However, at higher power the values of σ_{1f} are much higher than one would calculate on the basis of a simple two-fluid model in which the total number of carriers is constant so that the decrease in n_s with v_s results in a corresponding increase in the density of normal electrons. This gives a formula for J_1 in terms of v_s which corresponds to Eq. (7). A formula for σ_{1f} in terms of α can then be derived to the same approximation as Eq. (12).

$$\sigma_{1f}/\sigma_1=1+[n_s(0)/n-n_s(0)](1/16)\alpha^2. \qquad (13)$$

Calculations based on this model give values of σ_{1f} which are much smaller than we observe. In fact, when $\alpha=1$ in Fig. 3 the experimental ratio of σ_{1f} to σ_{2f} indicates that the loss is about a third of the energy stored in the superfluid so that the conditions under which Eq. (7) was derived may not be met.

The anomalies in σ_{1f} are strikingly indicated in Fig. 5 where σ_{2f}/σ_2 and σ_{1f}/σ_N have been plotted as a function of relative transmitted power for one film at three different temperatures. The vertical dashed line indicates the point at which $|J_2|\cong J_c$. At higher temperatures the departure of σ_{2f} from theory occurs when $|J_2|$ is less than J_c which is consistent with the observation of a higher relative loss $(\sigma_{1f}/\sigma_{2f})$ at higher temperatures. Of particular significance is the peak in σ_{1f} which is nearly 7 σ_N at the lowest temperature. It is

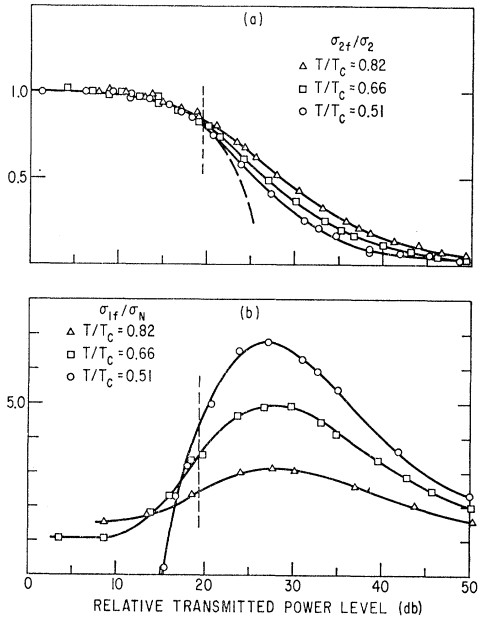

FIG. 5. Electric field dependence of the fundamental conductivity at different temperatures. Film 3 of Table I. $T/T_c=0.82$, $\sigma_2/\sigma_N=4.9$; $T/T_c=0.66$, $\sigma_2/\sigma_N=11.3$; $T/T_c=0.51$, $\sigma_2/\sigma_N=16.5$.

tempting to identify this peak with the peak in the temperature dependence of σ_1 calculated from the BCS theory,[21] but this peak would be less than 2 σ_N for the values of T_c and ω in our measurements. The BCS calculation does give a larger value of σ_1 and, consequently, a steeper rise of σ_{1f} with transmitted power, but the values of σ_{1f} are still substantially smaller than we observe. We conclude that a two-fluid model is inadequate to describe the behavior of these films in high electric fields.

B. High-Power Region ("Domain Growth")

So far, the experimental results have been analyzed in terms of a two-fluid model in which the electromagnetic properties of the superconducting film are described by a complex conductivity. The results of such an analysis are shown in Fig. 6(a) where σ_{2f}/σ_N and σ_{1f}/σ_N are plotted as functions of the input attenuator setting for a single film at a low temperature. Since we actually measure the amplitude and phase of the fundamental TE_{10} component of the transmitted field, however, it is clear that, *a priori*, we can fit our results with any two-parameter model.

Another model which seems more reasonable at higher power levels is shown in Fig. 6(b). Here the electrodynamic properties of the superconducting film are represented by a series circuit rather than the parallel circuit which corresponds to the two-fluid model. If, for example, the current-carrying superconducting state is unstable against the formation of domains,[23] the growth of normal strips perpendicular to the electric field would provide a physical basis for this representation. In this picture, r_f and x_f would be related to the fractions of the film which are normal and superconducting, respectively. Note that the anomalous peak in σ_{1f} is replaced by a monatonic rise in r_f, and there is an initial maximum in x_f. The fact that this initial rise in x_f can be interpreted as a decrease in σ_{2f} indicates that the two-fluid model provides a reasonable picture of the early stages of the nonlinearity.

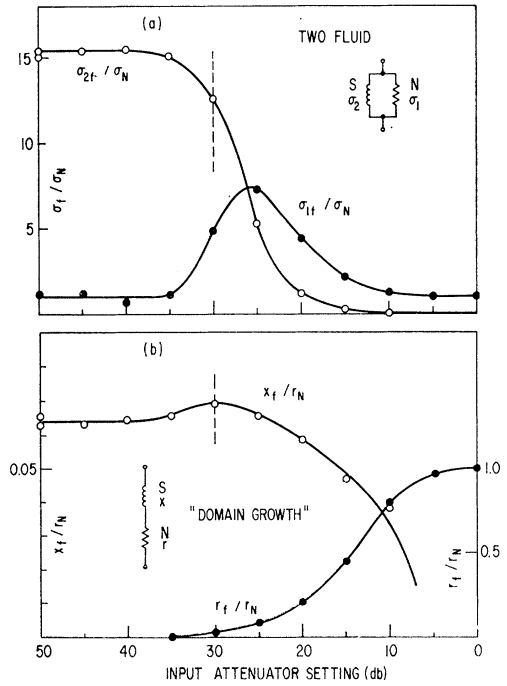

FIG. 6. Two interpretations of the nonlinear electrodynamics of superconducting films. Film 2 of Table I. $T/T_c=0.66$. (a) Two-fluid model; (b) series or domain-growth model.

The series and parallel models can be distinguished experimentally by their dc response when microwave pulses are transmitted through the film. If the two-fluid model applies, the normal fluid will be short-circuited by the superfluid, and a dc voltage will not appear across the film until it is fully normal. On the other hand, if the series model applies, the fraction of the film which is normal will support a dc voltage, and the transmission of microwave pulses through the film should produce pulses of dc voltage across the film. Moreover, the height of the voltage pulses should increase in proportion to the growth of r_f.

To test this hypothesis dc measurements using a 0.1-mA current i_{dc} were made on two of the films listed in Table I.[24] The experimental arrangement is indicated schematically in Fig. 7. Because of the nonuniform distribution of electric field across the waveguide the films were scribed as shown in Fig. 7. This allowed observation of the dc voltage in the central region where the maximum effect was expected. In the transition region and below T_c dc voltage pulses were detected across both films. When the sample was in direct contact with the liquid helium, the dc pulses had the same shape as the microwave pulses over the whole power range. When the film was cooled only by helium vapor and the microwave power was large, the dc pulse decayed slowly. At the highest powers the decay time

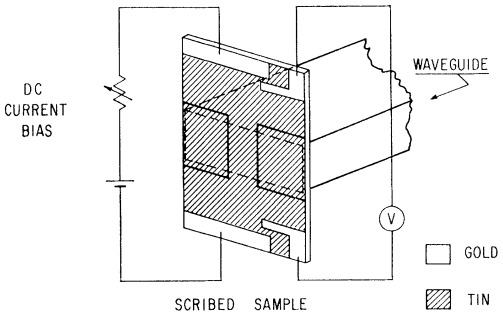

FIG. 7. Schematic diagram of experimental arrangement for measurements of dc voltage pulse. For most measurements the voltmeter V was replaced by a pulse amplifier and oscilloscope. $i_{dc}=10^{-4}$ A.

[23] Conference comment by J. Bardeen, Rev. Mod. Phys. **36**, 280 (1964).

[24] K. Rose and M. D. Sherrill, Bull. Am. Phys. Soc. **10**, 345 (1965).

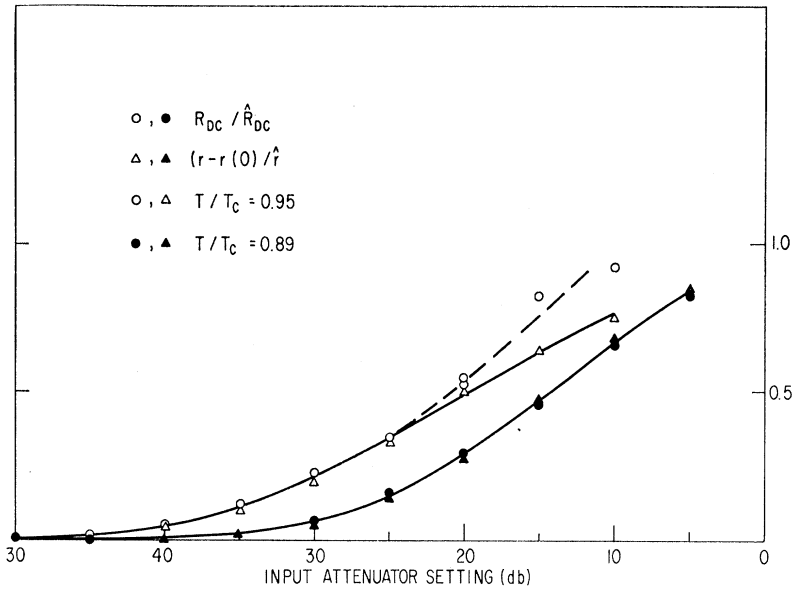

FIG. 8. Comparison of dc resistance and fundamental resistance as determined from microwave transmission in domain-growth region. Film 2 of Table I. $\hat{R}_{dc}$ and $\hat{r}_f$ are the peak experimental values.

was sometimes more than a millisecond. This shows that unless the sample makes good thermal contact with the bath heating effects play a major role.

Figure 8 shows the results of measurements of v_{dc}, the dc voltage pulse, and microwave transmission at two temperatures for the film whose unscribed behavior was shown in Fig. 6. $R_{dc}=v_{dc}/i_{dc}$ and the deviation of r_f from its low-power value are plotted, normalized to their maximum experimental values, as a function of input-attenuator setting. $R_{dc}/\hat{R}_{dc}$ increases monatonically with increasing incident power as predicted and, with this normalization, agrees well with the variation of $[r_f-r(0)]/\hat{r}_f$ at low-power levels. At high-power levels we would not expect these curves to agree since the growth of normal regions across the waveguide would affect r_f and R_{dc} differently. At lower temperatures the leakage of microwave power through the scribed regions dominates the transmission making it difficult to draw conclusions.

Most of the third-harmonic power is generated in the high-power region where the film's behavior is dominated by r_f. This is shown in Fig. 9 where both third-harmonic power and r_f are shown as functions of the incident microwave power. Since $x_f \ll r_f$ in the high-power region we should attribute most of the harmonic generation to rapid variations in the resistive domain structure.

The extent to which these results, particularly the appearance of domains, are influenced by film structure should be determined by further experiments.

VI. SUMMARY

We find that the nonlinear electrodynamics of these films are characterized by two distinct phenomena. At relatively low power there is a region in which the superelectron number density appears to decrease with

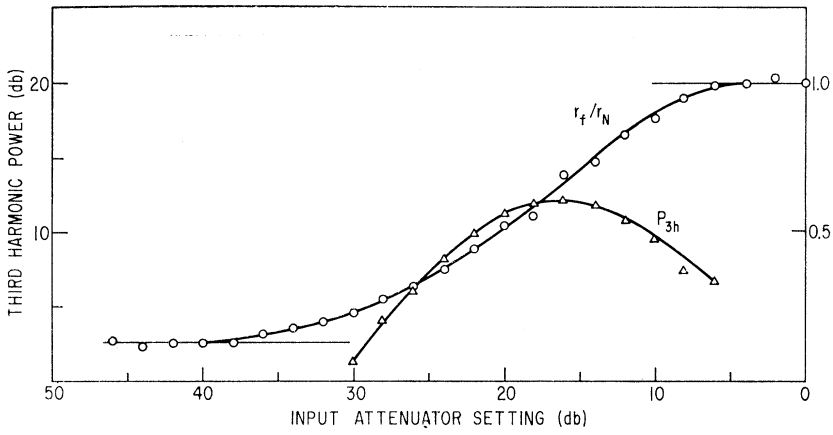

FIG. 9. Comparison of 3rd-harmonic generation and growth of fundamental resistance. Film 1 of Table I. r_N corresponds to σ_N.

supervelocity as described by the Ginsburg-Landau theory. The observed losses are, however, too large to be explained by a two-fluid model. They seem to be caused by the appearance of regions of normal resistance which neither the 9.4-Gc/sec current nor direct current can avoid.[8] These regions of normal resistance dominate the behavior of the films at high power and are responsible for most of the third-harmonic generation.

PHYSICAL REVIEW VOLUME 145, NUMBER 1 6 MAY 1966

Paramagnetic Resonance of Divalent Praseodymium in Calcium Fluoride

F. R. MERRITT, H. GUGGENHEIM, AND C. G. B. GARRETT
Bell Telephone Laboratories, Murray Hill, New Jersey
(Received 20 December 1965)

The electron paramagnetic resonance spectra of Pr^{++} in the cubic field of CaF_2 was obtained at 24 kMc, at liquid-helium temperatures. As predicted by Lea, Leask, and Wolf, the measurements show that the ground state of Pr^{++} is Γ_8. We estimate their parameter x to be -0.55 for Pr^{++}, which is in line with data on other ions in CaF_2. Extensive and complicated hyperfine structure was detected in addition to the fine-structure splitting of the Γ_8 state but no analysis is made of it. Since the hyperfine splitting was not small relative to the Zeeman splitting, normally forbidden $\Delta m_I = \pm 1$ transitions were also observed.

INTRODUCTION

THERE has been interest and controversy[1,2] with regard to the question of the paramagnetic resonance spectrum of trivalent Nd on cubic sites in calcium fluoride. In the hope of illuminating this topic, we present here paramagnetic resonance data on the isoelectronic ion Pr^{++} on cubic sites in the same crystal. The measurements show that the ground state of Pr^{++} is Γ_8, as predicted by Lea, Leask, and Wolf[3]; our estimate of the parameter x defined by Lea, Leask, and Wolf is -0.55, which appears to be more consistent with data on other ions in CaF_2 than is Vincow and Low's estimate $x=-1.0$ for Nd^{3+}. In addition to the fine-structure splitting of the Γ_8 state, our experiments show an extensive and complicated hyperfine structure which has not yet been analyzed in detail.

EXPERIMENTAL DETAILS

Calcium fluoride crystals containing 0.1% Pr, obtained from Optovac Inc., were heat-treated in an electric field[4] to convert some fraction of the Pr^{3+} into Pr^{++}. Cube-shaped oriented single crystals $\sim$1.5 mm on a side were centered along the axis of a cylindrical TE_{011} cavity, arranged in such a way that the applied magnetic field, when rotated in a major crystal plane, was always normal to the rf magnetic field. Orientation was done by x-ray techniques, with an estimated over-all accuracy of $\pm 1°$. Experiments were carried out at liquid-helium temperatures using a superheterodyne paramagnetic resonance spectrometer operating at K band (1.25 cm). The maximum available magnetic field was 16.4 kG.

RESULTS

Measurements at 1.4°K showed in most orientations two sets of six resonance lines, which were characterized by a highly anisotropic behavior. The angular dependence of the pattern indicated cubic symmetry. In certain directions five additional lines were observed, at fields intermediate between the original six. In most directions where they were observed, these additional lines were considerably weaker than the original six, but over some ranges of angle the order of intensities was reversed. The angular dependence of intensities was in fact quite complicated, and, even in crystals where the signals were strongest, there were orientations where some of the lines were too weak to detect. Figures 1 and 2 illustrate the data.

The width of each line at 1.4°K was around 100 G. The lines broadened with increasing temperature, but could still be detected at 4.2°K.

The presence of this spin-resonance spectrum was definitely associated with the depth of coloring of the crystal. The lines were stronger in the more deeply colored crystals. Furthermore, in one crystal, in which the electrolysis was incomplete so that coloring was restricted to about one-half of the crystal, a sample cut from that half showed the resonance pattern while the other half did not.

ANALYSIS OF DATA

The correlation between the strength of the coloring of the crystal and the resonance pattern, the number of lines in the hyperfine structure, and the 90° symmetry of the anisotropy all point to the assignment to divalent

[1] G. Vincow and W. Low, Phys. Rev. **122**, 1390 (1961).
[2] W. P. Wolf, J. Phys. Soc. Japan, Suppl. B-I **17**, 442 (1962).
[3] K. R. Lea, M. J. M. Leask, and W. P. Wolf, J. Phys. Chem. Solids **23**, 1381 (1962).
[4] H. Guggenheim and J. V. Kane, Appl. Phys. Letters **4**, 172 (1964).